# Turning Lignin into Aliphatic Organic Chemicals in Gamma-Valerolactone: Advances into a Bioelectrorefinery

Lucie M. Lindenbeck,[a,b] Sira Dahlhaus,[a] Luca M. Wende,[c] Björn B. Beele,[a] Nils Helge Schebb,[c] Christian W. Lehmann,[b] Julia Bornhorst,[c] Adam Slabon,[a,d]* and Bruno V. M. Rodrigues[a]*

[a] Chair of Inorganic Chemistry, Faculty of Mathematics and Natural Sciences, University of Wuppertal, Gaußstraße 20, 42119 Wuppertal, Germany

[b] Max-Planck-Institut für Kohlenforschung, Kaiser-Wilhelm-Platz 1, 45470 Mülheim an der Ruhr, Germany

[c] Chair of Food Chemistry, Faculty of Mathematics and Natural Sciences, University of Wuppertal, Gaußstraße 20, 42119 Wuppertal, Germany

[d] Wuppertal Center for Smart Materials & Systems, University of Wuppertal, 42119 Wuppertal, Germany

**ABSTRACT:** This investigation reports on the reductive electrochemical depolymerization and dearomatization of lignin using water/γ-valerolactone (GVL) as solvent system combined with sodium carbonate as electrolyte. GVL, derived from biomass, has often served as a solvent for biomass treatment, such as in the Organosolv process. Consequently, various strategies for biorefineries have emerged, utilizing GVL as a green platform, with a primary focus on its potential for the delignification of lignocellulosic biomass when combined with water and dilute acid. This investigation proposes the electrochemical depolymerization of lignin in GVL as a step toward the concept of a bioelectrorefinery, valorizing lignin conversion into aliphatic organic chemicals. Applying a current of −100 mA over 8 h resulted in the formation of sodium levulinate, sodium 4-hydroxyvalerate, sodium acetate, and sodium formate, as confirmed by liquid chromatography electrospray ionization high resolution mass spectrometry (LC-ESI-HRMS), nuclear magnetic resonance (NMR), and infrared (IR) spectroscopy. These findings enhance the understanding of GVL as a biomass-based platform, showcasing its potential as a medium in the conversion of lignin into valuable aliphatic organic chemicals. This study contributes to advancing the bioelectrorefinery concept and opens new avenues for utilizing renewable resources, envisioning the feasible future replacement of crude oil as the primary industrial source of carbon-based chemicals.

## INTRODUCTION

The prevailing climate crisis is compelling industries to adopt more sustainable processes. These processes must ensure efficient resource utilization, minimize waste production, and substitute fossil fuels with renewable energy sources. Although the chemical industry is vital for pharmaceuticals and polymers, traditional processes are often not aligned with environmental concerns. [1] Historically, the industry has relied heavily on oil and gas due to their availability and cost-effectiveness. [2] However, with fossil fuels depleting and energy demand rising, the focus has shifted to renewable sources such as wind, solar, geothermal, hydropower, and biomass - a readily available organic carbon source of high interest. [3]

The conversion of biomass and biomass waste into fuels and chemicals is a promising route toward a more sustainable economy. About 170 billion tons of renewable resources are generated on Earth every year, but only 3.5% of this amount is accounted for human use. [4] Concerning lignocellulosic biomass, lignin, one of its main components, has emerged as a valuable raw material for the production of chemicals and fuels. [5] As a complex biomacromolecule found in plant cell walls, lignin provides structural support to plants and is highly abundant in lignocellulosic biomass, particularly in wood. It can be sourced from various materials, including hardwood, softwood, and agricultural residues. The highly crosslinked molecular structure of this polyphenol involves three primary phenylpropane units interconnected by ether and carbon-carbon linkages, along with hydroxyl and methoxy groups, which accounts for its recalcitrant characteristic. [6,7] Therefore, the selective and efficient breakdown of this macromolecule into high-value added products is rather challenging. [5]

Depolymerizing lignin requires efficient catalysts and optimized reaction conditions. Precise adjustment of parameters such as temperature, pressure and choice of solvent is critical to achieving high product yields. [6,8–11] In electrochemical approaches, the selectivity and speed of the reaction can be improved by adjusting the potential or current density, as well as other parameters such as solvents, electrolytes, and electrode materials. [12–17] Various sustainable conversion approaches, including biological, [18–23] thermal, [8] chemical, [9–11] and electrochemical [12–16,24,25] pathways have
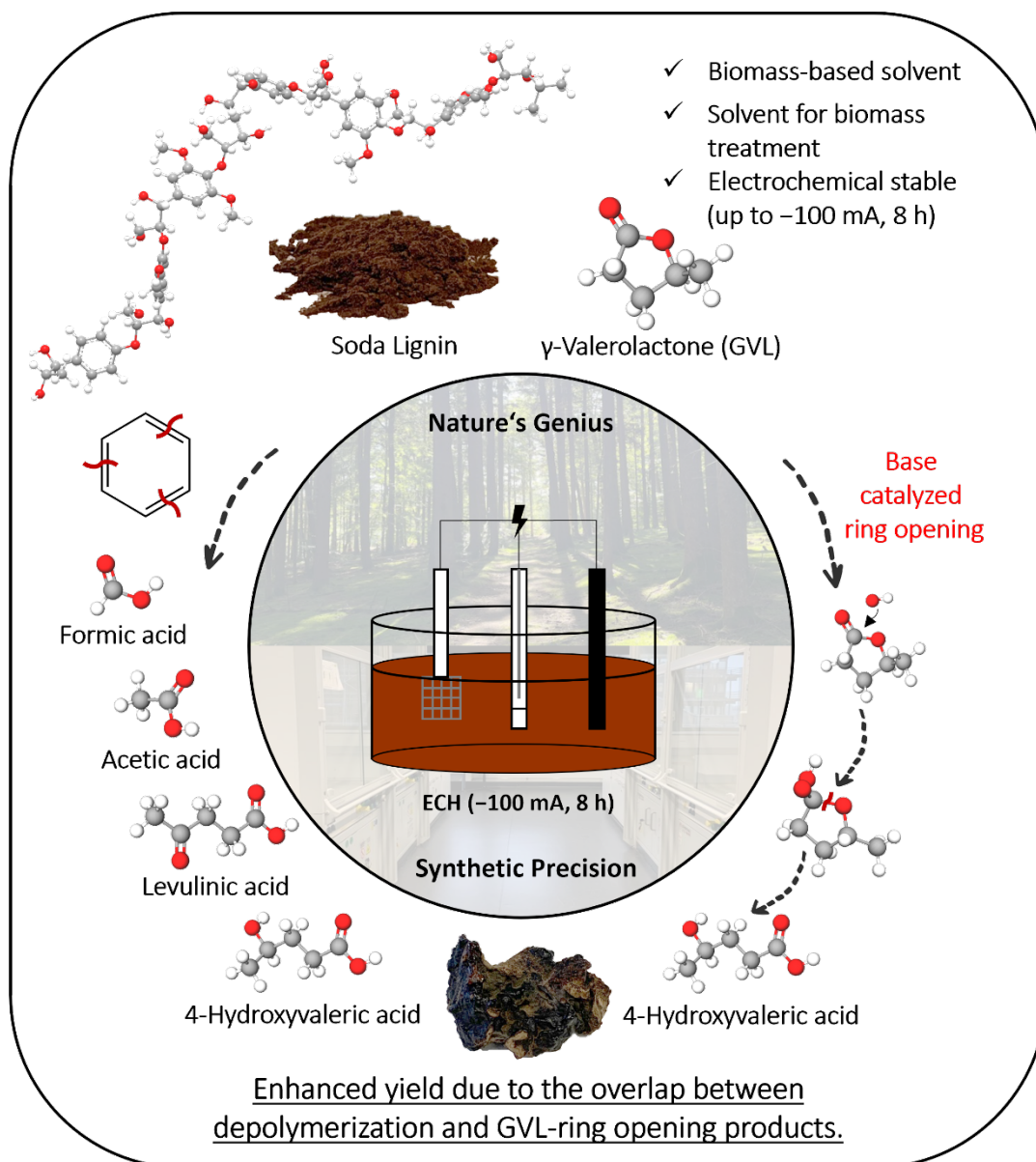
**Scheme 1.** Scheme of the electrochemical depolymerization of soda lignin in a water/GVL system using electrocatalytic hydrogenation (ECH). The main depolymerization products (DL) of this process are levulinic acid, 4-hydroxyvaleric acid, formic acid, and acetic acid. Additionally, 4-hydroxyvaleric acid is synthesized by the ring-opening reaction of the GVL, which enriches the products of depolymerization and increases the reaction yield.

been explored in order to attempt to break down lignin into smaller (aromatic) compounds. [26] In this context, electrochemical processes have gained a significant recognition in recent decades, [27,28,29] due to the possibility of using milder conditions while being atom-efficient. [30] Electrochemical biomass depolymerization aligns with *Green Chemistry* principles introduced in the early 1990s as the "design of chemical products and processes to reduce or eliminate the use and generation of hazardous substances". [31] Electrocatalysis can operate at ambient temperature and pressure, overcoming kinetic barriers through an applied potential rather than thermal energy, [32] with the advantage of using hydrogen and oxygen produced from water splitting. [33] The sustainability aspect can be further increased by using bio-

mass-derived electrodes, such as carbon, and renewable energy sources, such as solar energy. [34] In addition, heterogeneous catalysis enables simple product-catalyst separation.

Lignin depolymerization through electrochemical processes has been recently documented using many eco-friendly solvents, such as levulinic acid, [12] ionic liquids (e.g., 1-ethyl-3-methylimidazolium trifluoromethanesulfonate and triethylammonium methanesulfonate), [35,36] deep eutectic solvents (DES), [37] and aqueous sodium carbonate ($Na_2CO_3$) solvent system [16]. After a 20 h depolymerization reaction of lignin at −1.7 V with a copper electrocatalyst in levulinic acid, monomers and dimers could be obtained in which aryl ether and phenol groups predominated. [12] Using triethylammonium methanesulfonate as a protic ionic liquid and a $Ru_{0.25}V_{0.05}Ti_{0.7}O_x$ mixed oxide electrode, various oxidation products, including aldehydes (benzaldehyde, 3-

furaldehyde, m-tolualdehyde, vanillin, and acetovanillon) and ketones, were obtained at potentials ranging from 1.0 V to 1.5 V. A yield of 6 wt.% of the original lignin mass was achieved. [36] During the electrochemical depolymerization of lignin in a DES at different potentials (0.5 V and 1 V), guaicol, vanillin, acetovanillon, and syringaldehyde were obtained as the main products. Compared with the amount of lignin used, a yield of 2 wt.% was obtained. [37] In the process of depolymerizing with simultaneous dearomatization of lignin within an aqueous $Na_2CO_3$ solvent system, four aliphatic main products were identified: sodium levulinate, sodium 4-hydroxyvalerate, sodium acetate, and sodium formate. These products were obtained after 20 h at a current of −175 mA under reductive conditions. A yield of 58 wt.%, relative to the initial mass of lignin, was achieved. [16]

Solvent choice is a crucial aspect of *Green Chemistry*. [38,39] In this context, biomass-derived γ-Valerolactone (GVL) has been proved to be a sustainable solvent, since it boasts favorable physical and chemical properties and can be stored and transported in large quantities with ease and safety, thanks to its low melting (−31 °C), high boiling (207 °C) and flash (96 °C) points. GVL has a distinct odor, aiding leak detection, and excellent miscibility with water, promoting biodegradation. While serving as a polar aprotic solvent, GVL plays a pivotal role in stabilizing acidic protons derived from protonated transition states. This property accelerates the rates of acid-catalyzed biomass conversion reactions. [40] Utilized either as a primary solvent or co-solvent, GVL demonstrates its versatility in generating higher-value products from diverse sources such as lignin, carbohydrates, sugars, and smaller molecules. The combination of GVL with water creates arrangements at the surface that effectively promote hydrolysis reactions. [41] An intriguing application of GVL lies in its role as a solvent for the Organosolv treatment. This application not only prevents the reprecipitation of lignin by-products on cellulose surfaces but also augments chemical modifications at the cellulose surface, including bond cleavage. [41] Positioned as a promising solvent within a biorefinery aspiring for circularity, GVL's widespread adoption hinges on the feasibility of large-scale production to drive down costs. [42] Noteworthy initiatives in this direction are emerging from various European countries. [43]

This study builds upon our experience in the electrocatalyzed depolymerization and dearomatization of lignin aqueous system using $Na_2CO_3$ as an electrolyte, [16] which generates sodium levulinate, sodium 4-hydroxyvalerate, sodium acetate, and sodium formate as the major depolymerization products (DL). [16] At the same time, given that GVL has been often used for the delignification and pretreatment of the lignocellulosic biomass, [44] the utilization of this solvent as medium for the electrocatalytic depolymerization of lignin becomes appealing. It is known that GVL undergoes a ring-opening reaction to 4-hydroxyvalerate under basic conditions. [45,46] This could for instance result in an overlap between the products of lignin depolymerization in water/ $Na_2CO_3$ and the ring-opening product of GVL. The main goal of this study was to increase the overall yield of the reaction by selectively inducing the ring opening of GVL to enrich the depolymerization products with 4-hydroxyvalerate (*Scheme 1*). These discoveries deepen our comprehension of GVL's role as a biomass-derived platform, highlighting its capacity as a medium for transforming lignin into valuable aliphatic organic chemicals. This research not only propels the bioelectrorefinery concept forward but also paves the way for harnessing renewable resources, foreseeing a plausible shift from crude oil to become the predominant industrial source for carbon-based chemicals in the future.

## MATERIALS AND METHODS

### Materials

γ-Valerolactone (GVL, thermo scientific) (98 %), $Na_2CO_3 \times 10\ H_2O$ (Grüssing GmbH), and levulinic acid (Merck KGaA) (98%) were used as received. The soda lignin used originates from the hardwood black liquor of a sulphur-free pulp production in a pilot plant (WAT Venture Sp. z o.o., Poland). All aqueous solutions were prepared with ultrapure water obtained from a Millipore system.

### Electrochemical Depolymerization of Soda Lignin

Soda lignin was dissolved at 3 g $L^{-1}$ in 50 mL of a 5 M GVL aqueous solution by magnetic stirring. Electrochemical depolymerization was conducted using a three-electrode setup on an ATLAS 1131 Electrochemical Unit & Impedance Analyser (Atlas-Sollich, Rebiechow). The three-electrode set-up consisted of a carbon working electrode, a platinum wire counter electrode, and an Ag/AgCl (saturated KCl) reference electrode. 5 mL of a sodium carbonate solution (1 M) was added to the solution as an electrolyte. Chronopotentiometry was performed using an applied current of −100 mA for 8 h at room temperature. After the reaction, a brown, but slightly transparent solution remained. Water was removed from the mixture under reduced-pressure conditions, leaving behind a solid and liquid, which were separated from each other by filtration. The solid was then redissolved in water, which was once again removed under reduced pressure. This procedure was repeated several times. The resulting brown solid was dried at 60 °C in a drying oven.

^{1}H NMR (600.13 MHz, $D_2O$) δ 8.49 (s, formate), 4.89 – 4.81 (m, GVL), 3.85 (h, 4-hydroxyvalerate), 2.81 (t, levulinate), 2.74 – 2.62 (m, GVL), 2.49 – 2.39 (m, GVL), 2.44 (t, levulinate), 2.34 – 2.21 (m, 4-hydroxyvalerate), 2.26 (s, levulinate), 1.95 (s, acetate), 1.75 (dtd, 4-HVA), 1.43 (d, GVL), 1.21 (d, 4-hydroxyvalerate).

IR (Diamond-ATR): ν [$cm^{-1}$] = 3381 (OH, w), 3201 (OH, w), 2962 (CH, w), 2930 (CH, w), 2916 (CH, w), 2872 (CH, w), 1773 (C=O, w), 1707 (C=O, w), 1561 (COO⁻, vs), 1406 (COO⁻, s), 1367 (m), 1312 (m), 1296 (w), 1193 (w), 1127 (m), 1073 (m), 1051 (w), 938 (w), 920 (w), 873, 846 (w), 796, 781 (w), 766 (w), 691 (w), 649 (w), 621 (w), 593 (w), 551 (w), 516 (w), 467 (w), 433 (w).

### Synthesis of sodium 4-hydroxyvalerate

Sodium 4-hydroxyvalerate was synthesized according to previous works. [16]

^{1}H NMR (600.13 MHz, DMSO-d[6]) δ 6.27 (s, 1H, OH), 3.60 (h, $^3J_{HH}$ = 6.0 Hz, 1H, C(OH)H), 2.10 (dt, $^2J_{HH}$ = 15.6, $^3J_{HH}$ = 6.4 Hz, 1H, CH₂), 2.03 (dt, $^2J_{HH}$ = 15.2, $^3J_{HH}$ = 7.1 Hz, 1H, CH₂), 1.50 (q, $^3J_{HH}$ = 6.3 Hz, 2H, CH₂), 1.00 (d, $^3J_{HH}$ = 6.2 Hz, 3H, CH₃).

^{13}C NMR (151 MHz, DMSO-d[6]) δ 178.43 (COO⁻), 66.99 (C(OH)H), 35.67 (CH₂), 35.31 (CH₂), 24.04 (CH₃).

IR (Diamond-ATR): ν [cm⁻¹] = 3383 (OH, w), 3236 (OH, w), 3151 (OH, w), 2962 (CH, w), 2930 (CH, w), 2916 (CH, w), 2884 (CH, w), 1562 (COO⁻, s), 1406 (COO⁻, s), 1367 (m), 1313 (m), 1295 (m), 1223 (w), 1194 (w), 1128 (m), 1073 (s), 1051 (m), 950 (m), 938 (m), 920 (m), 873 (m), 845 (w), 796 (w), 760 (w), 737 (w), 722 (w), 680 (w), 622 (w), 592 (w), 551 (w), 477 (w), 433 (w).

## Material characterization

**Vibrational spectroscopy**: FTIR spectra were measured using a diamond 7 ATR unit on a Nicolet ID5 in the range of 4000-400 cm⁻¹.

**Nuclear Magnetic Resonance Spectroscopy**: Nuclear magnetic resonance (NMR) measurements were performed on a BRUKER Avance 400 MHz spectrometer and on a BRUKER Avance III 600 MHz spectrometer. The following probe heads were used: 5 mm broadband inverse probe with automatic frequency determination, 5 mm QNP probe, and 5 mm broadband inverse probe. Chemical shifts were referenced with respect to Me₄Si.

**LC-ESI-HRMS:** Samples were dissolved in $H_2O$/ACN 50/50 ($v/v$) (1 μg mL⁻¹) and injected (5 μL) into the LC-ESI-HRMS system. Standard compounds were injected in a concentration of 1 μM. Chromatographic separation was carried out using a ZORBAX Eclipse Plus C18 column (2.1x150 mm; 1.8 μm) and A: $H_2O$/ ACN/HAc (95/5/0.1) ($v/v/v$) and B: ACN + 0.1% HAc as eluents at a flow rate of 300 μL min⁻¹. The LC-System was coupled to a QExactive HF Orbitrap mass spectrometer (Thermo, Schwerte, Germany) equipped with a HESI II ionization source operating in ESI(-) and ESI(+)mode with the following settings: sheath gas flow rate 48 psi; aux gas flow rate 11 arb; sweep gas flow rate 2 psi; spray voltage ±4.5 kV; capillary temperature 256 °C; S-lens RF level 75; aux gas heater temperature 413 °C. Data was acquired in Full MS/data dependent MS² mode with the following settings: Full MS: Resolution 120,000; AGC target 1x10⁶ ; Maximum IT 160 ms; Scan range $m/z$ 80-1000. ddMS² : Resolution setting 15,000; AGC target 5x10⁴ ; Maximum IT 100 ms; Top N 10; NCE 30.

**Scanning Electron Microscopy (SEM):** Micrographs of the electrodes were taken using a Hitachi TM3030 PLUS tabletop scanning electron microscope operated at an acceleration voltage of 15 kV. Backscattered electrons (BSE) and secondary electrons (SE) were detected to obtain both compositional distribution and topographic information.

## RESULTS AND DISCUSSION

In two recent investigations from our research group, the electrochemical depolymerization of technical lignins in different aqueous solvent systems have been reported, one comprising levulinic acid [12] and another based on a sodium carbonate ($Na_2CO_3$) aqueous solution. [16] Although γ-valerolactone (GVL) has been faced as a promising sustainable platform for biomass treatment and dissolution, this solvent undergoes a ring-opening reaction depending on the temperature and presence of acids or bases. [46,47] Wong *et al*. [46] investigated the stability of GVL under neutral, acidic, and basic conditions and Granatier *et al*. [47] studied its

stability under pulping conditions. In our investigation, before using GVL as a solvent for electrochemical depolymerization, its stability was assessed. For this purpose, the stability of GVL in combination with $Na_2CO_3$ as electrolyte was tested under different conditions - room temperature and 60 °C and during electrochemical reactions at different applied currents. It was confirmed that GVL, in combination with $Na_2CO_3$, undergoes a ring-opening reaction leading to sodium 4-hydroxyvalerate (*Figure S9, Table S2*, in further discussion referred to as 4-hydroxyvalerate). The percentage of 4-hydroxyvalerate increased by increasing the temperature (*Figure S10, Table S2*).

At an applied current of −100 mA for 8 h, the ring opening reaction was caused exclusively by the presence of $Na_2CO_3$ and not by the applied current (*Figure S11, Table S3)*. With longer reaction times (20 and 24 h) and higher currents (reductive ones, such as −150 mA, −200 mA, and oxidative ones such as +200 mA), the concentration of 4-hydroxyvalerate increased (*Figure S12-S14, Table S3*). The highest concentration of 10.0 mol% was achieved after 20 h at an applied current of −100 mA (*Figure S13, Table S3)*. A detailed analysis of the stability is provided in the Supporting Information (SI).

In a previous study conducted by our group, the electrocatalyzed depolymerization of soda lignin in an aqueous $Na_2CO_3$ solution resulted in four main products: sodium levulinate, sodium 4-hydroxyvalerate, sodium acetate, and sodium formate. [16] This study served as the basis for our current research, where we strategically utilized the overlap between the depolymerization products and the products from the GLV ring-opening reaction. The aim was to enhance the overall yield of the reaction by selectively inducing the ring opening of GVL, thereby enriching the depolymerization products with 4-hydroxyvalerate. An important observation from the investigation into the electrochemical stability of GVL is the molar ratio of 4-hydroxyvalerate to GVL after 8 hours at −100 mA. This ratio was identical to that of the reference reaction conducted without electrochemical intervention, which stands at 2.5 mol%. This equivalence suggests that the ring-opening process of GVL is exclusively attributed to base catalysis under these conditions.
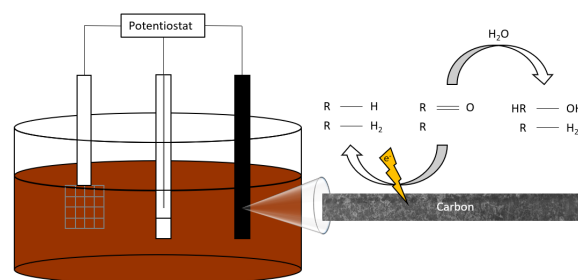


Figure 1. Reaction setup and possible mechanisms of electron transfer in ECH reaction on the carbon surface: electronation–protonation and electrocatalytic hydrogenation. A three-electrode setup consisting of a carbon working electrode, a platinum counter electrode, and Ag/AgCl (saturated KCl) is used for the reaction. The reaction solution consists of 5 M GVL, with a soda lignin concentration of 3 g L⁻¹. As electrolyte, 1 M $Na_2CO_3$ is added to the reaction solution.

The molar ratio of 4-hydroxyvalerate surpassed that of the reference reaction only when subjected to higher currents or prolonged reaction times. Therefore, we judiciously chose the parameters of −100 mA and an 8 h reaction time for the depolymerization process, since higher currents and/or longer reaction times would excessively promote the formation of sodium 4-hydroxyvalerate, reducing the influence of depolymerized products in the final product.
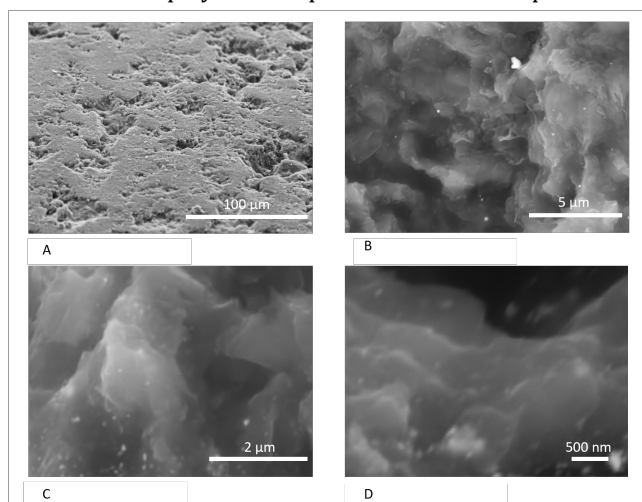


Figure 2. SEM micrographs of the carbon electrode at different areas and magnifications: **A** x1.0k, **B** x15.0k, **C** x40.0k, **D** x60.0k. The micrographs show an enlarged surface of the electrode, which is caused by its highly porous character.

The electrochemical depolymerization of soda lignin in GVL was carried out using a carbon working electrode, platinum counter electrode, and Ag/AgCl (saturated. KCl) reference electrode. The reaction setup and possible mechanisms of electron transfer in ECH reaction on the carbon surface are shown in *Figure 1*.

A current of −100 mA corresponded to a current density of −18 mA/cm². However, when observing the SEM micrographs of the carbon electrode (*Figure 2*), the actual surface area was assumed to be significantly larger due to intrinsic porosity. The chronopotentiometry course at −100 mA is shown in *Figure 3*. At the beginning of the reaction, a potential of −4.1 V was present which was reduced to an average potential of −3.7 V during the reaction.
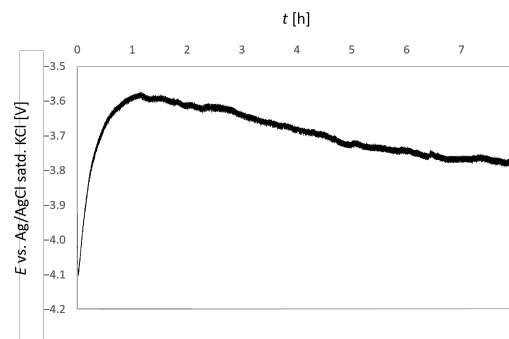


Figure 3. Potential (Ag/AgCl (saturated KCl)) *vs.* time during depolymerization of soda lignin in GVL at a constant current of −100 mA over a period of 8 h. Within the first hour, the potential decreases, whereupon it constantly increases over the next seven hours.
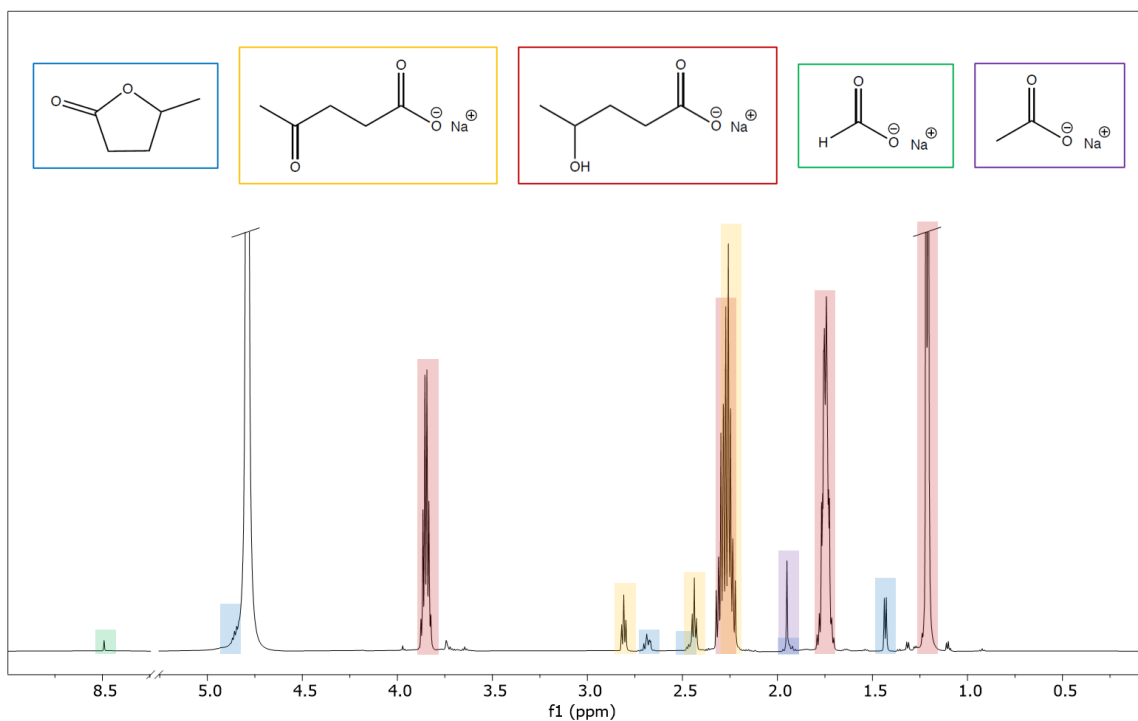


Figure 4. $^1$H NMR spectrum (D$_2$O, 600.13 MHz) of the depolymerization products (DL). Levulinate (yellow), 4-hydroxyvalerate (red), formate (green), and acetate (purple) can be identified as the main products of soda lignin depolymerization. GVL (blue) is also recognizable because of its equilibrium with 4-hydroxyvalerate in water.
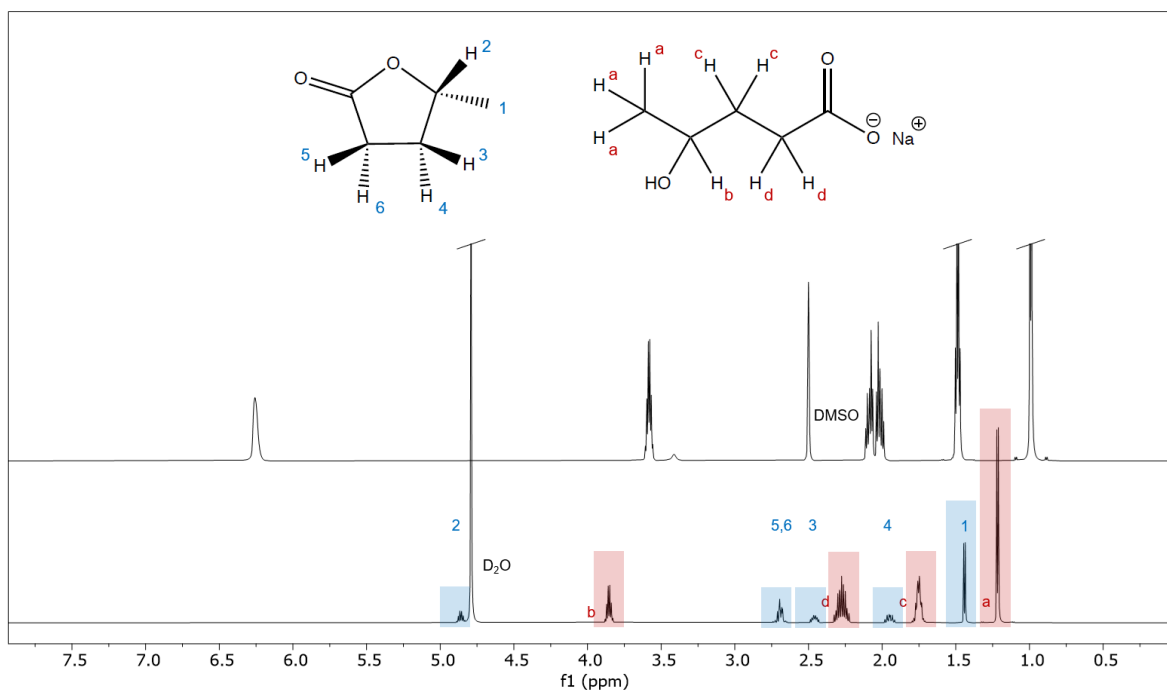
Figure 5. $^1$H NMR spectra (D$_2$O (below) and DMSO–d$^6$ (above), 600.13 MHz) of 4-hydroxyvalerate. A comparison of the measurements of the same product in two different solvents shows the equilibrium reaction between GVL and 4-hydroxyvalerate. In DMSO-d$^6$, only the signals of 4-hydroxyvalerate (red) are present. In D$_2$O, on the other hand, GVL (blue) signals are also present. Thus, the ring of GVL is closed again in equilibrium by dissolving sodium 4-hydroxyvalerate in water.
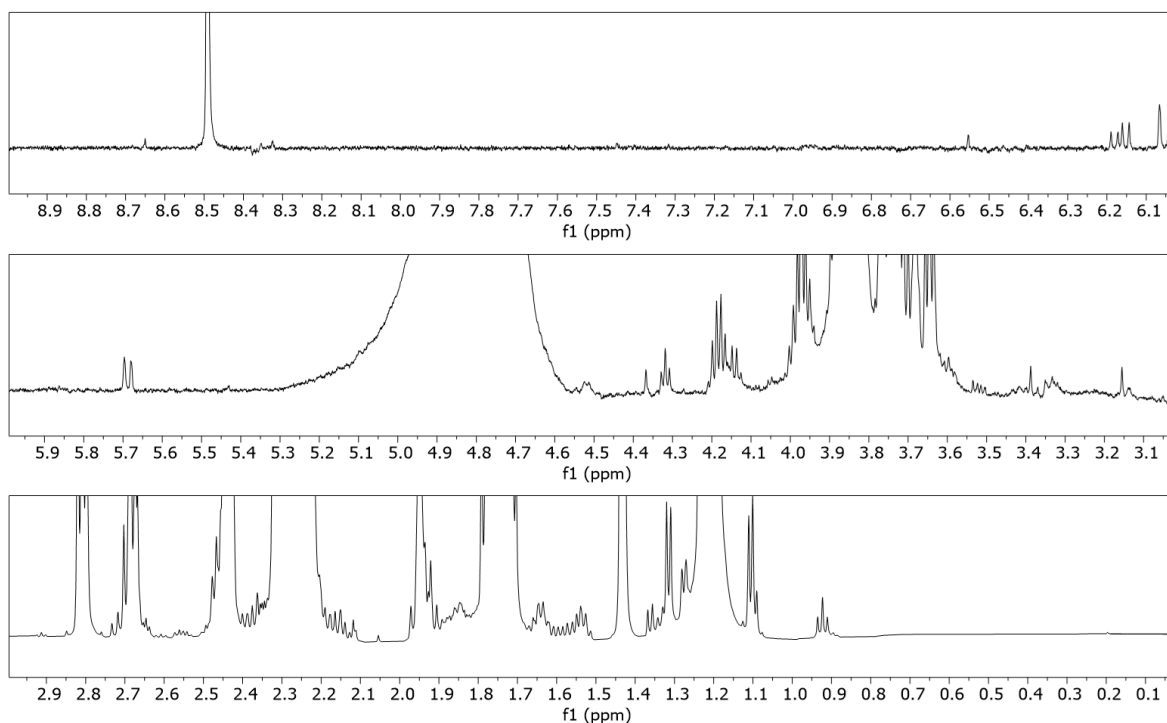


Figure 6. $^1$H NMR spectrum (D$_2$O, 600.13 MHz) of the DL - higher magnification.

In the first hour, the potential dropped to −3.6 V, slowly increasing to −3.8 V afterwards until the end of the reaction. This indicates that either part of the solvent began to evaporate, or the components of the reaction solution settled on the electrode. Both lead to the fact that a higher potential is necessary to maintain a constant current of −100 mA. During the reaction, the volume of the solution gradually
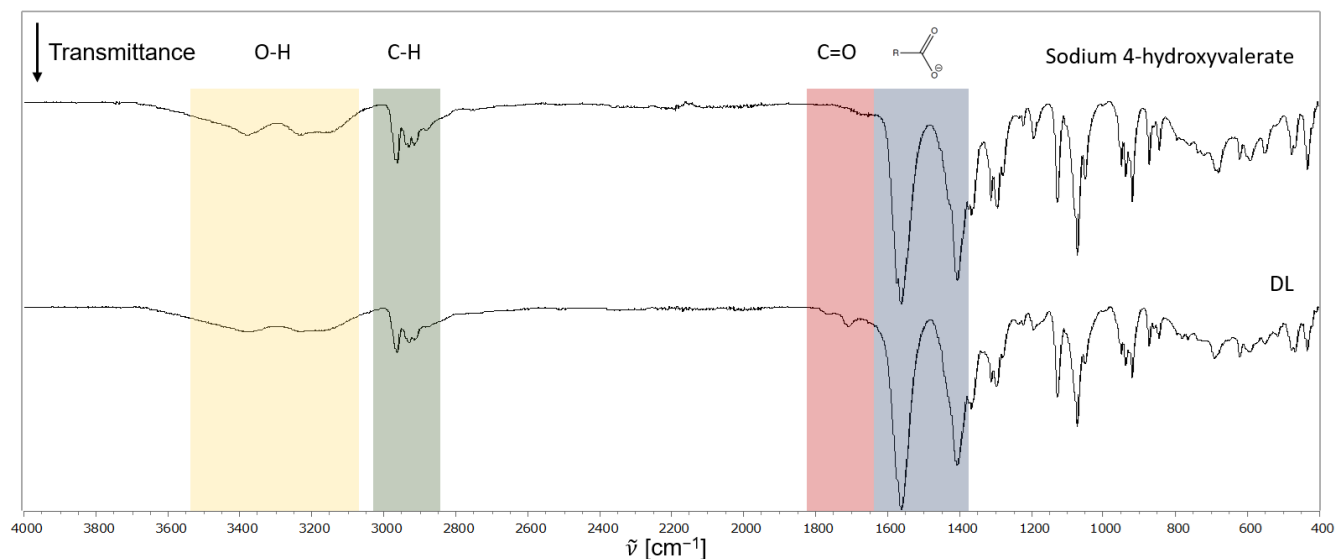
Figure 7. FTIR spectra of sodium 4-hydroxyvalerate and the DL. In the spectrum of sodium 4-hydroxyvalerate the characteristic bands (-OH, -CH and -COO⁻) are present. The spectrum of the DL shows the characteristic vibrations of the O-H, C-H, C=O, and COO⁻ groups. Sodium levulinate can also be identified as one of the main products contributing to the carbonyl vibration at 1707 cm⁻¹.

decreased. The water electrolysis process explains this phenomenon, which occurs at a high working voltages of $E$ >1.23 V *vs.* RHE and results in formation of hydrogen at the cathode and oxygen at the anode. [48] The remaining water was removed under reduced pressure after the reaction resulting in 1030 mg of a brown solid and 16.5 mL of a remaining liquid. The mass of products after depolymerization was seven times greater than the starting soda lignin. Accordingly, it can be assumed that the product was a mixture of the depolymerization products of soda lignin (DL) and the sodium 4-hydroxyvalerate, also generated by the lignin depolymerization process. This hypothesis was further supported by NMR, FTIR, and mass spectrometry.

The ^{1}H NMR spectrum of the DL (*Figure 4*) shows mainly the signals of 4-hydroxyvalerate and GVL. The ring opening and closing of GVL is an equilibrium reaction in water. For this reason, GVL can also be detected in ^{1}H NMR in $D_2O$ (*Figure 5*). In addition, levulinate signals are observed at 2.81, 2.44, and 2.26 ppm. [16] Moreover, two more singlets at 1.95 ppm and 8.49 ppm can be assigned to acetate and formate. [16] It is assumed that the products are the sodium salts of the carboxylic acids due to the use of $Na_2CO_3$ as electrolyte since no proton signals are recognizable in the ^{1}H NMR. These results are consistent with those of our previous study on the depolymerization and dearomatization of lignin in an aqueous $Na_2CO_3$ medium. [16]

The FTIR spectra of sodium 4-hydroxyvalerate and DL provide insights into their molecular structure. In the FTIR spectrum of sodium 4-hydroxyvalerate (*Figure 7*), OH vibration signals are evident between 3400-3100 cm⁻¹. CH vibration signals are observed at 2962, 2930, 2916, and 2884 cm⁻¹. Signals at 1562 (antisymmetric stretch vibration) and 1406 cm⁻¹ (symmetric stretching vibration) can be associated to the carboxylate group. [49]
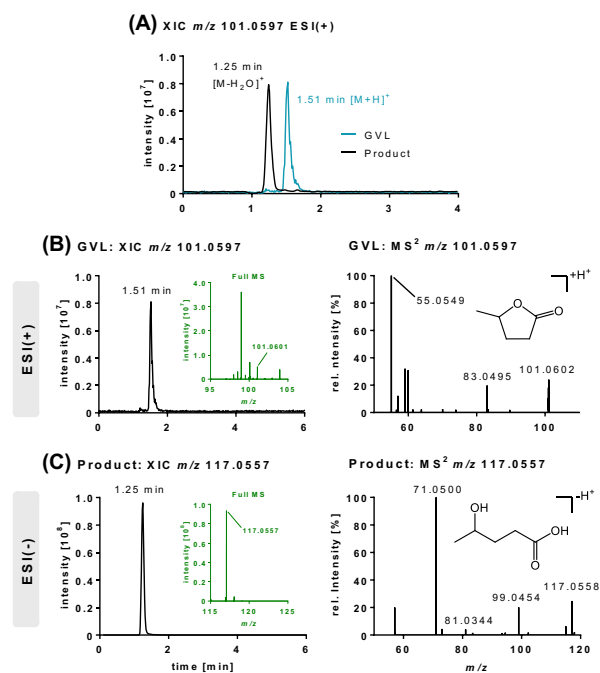


Figure 8. Characterization of GVL and its hydrolysis product 4-hydroxyvalerate using LC-MS. **(A):** Extracted ion chromatogram (XIC) at *m/z* 101.0597 of the [M+H]⁺ ion of GVL (blue) and the [M+H-H₂O]⁺ ion of the hydrolysis product in LC-ESI(+)-MS. **(B):** XIC at m/z 101.0597 showing the signal of GVL in addition to its Full MS and MS² spectra obtained in ESI(+). **(C):** XIC at m/z 117.0557 showing the signal of the [M-H⁺]⁻ ion of 4-HVA in the hydrolysis product and its Full MS and MS² spectra in LC-ESI(-)-MS.
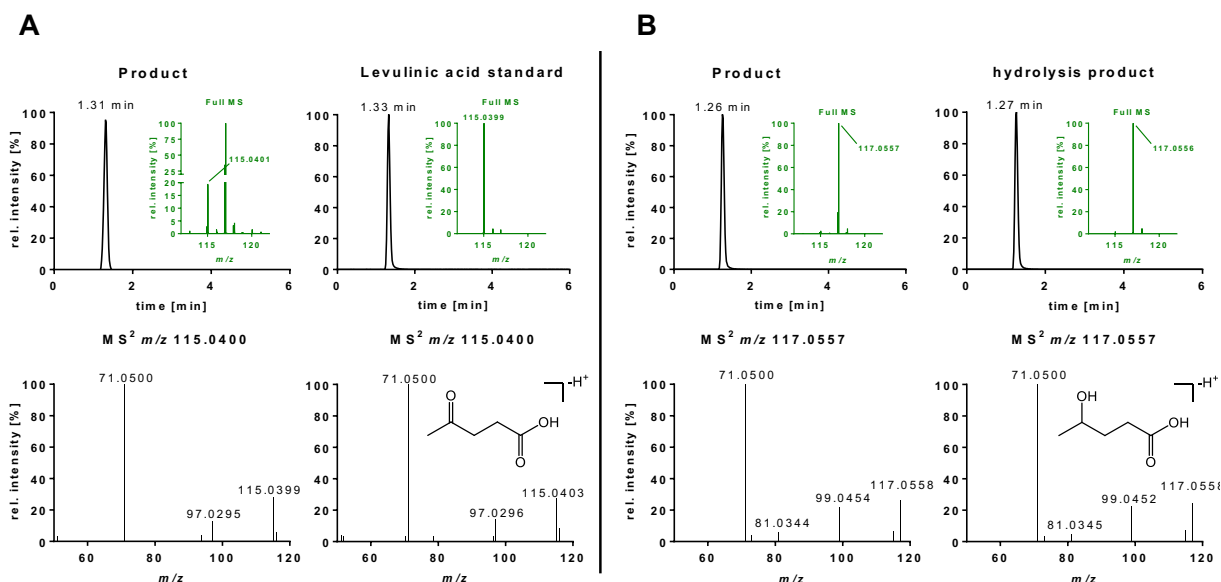
Figure 9. Detection of levulinic acid (**A**) and 4-hydroxyvalerate (**B**) in the depolymerization product using LC-ESI(-)-HRMS. **TOP**: extracted ion chromatogram and MS spectrum of **A:** the depolymerization product and a levulinic acid standard compound at $m/z$ 115.0400 and **B:** the depolymerization product and the hydrolysis product of GVL which was tentatively identified as 4-hydroxyvalerate at $m/z$ 117.0557 (Fig. S16). **Bottom**: corresponding fragment spectra. The peaks at 1.31 min and 1.26 min in the depolymerization product could be identified as [M-H+]- ion of levulinic acid at $m/z$ 115.0400 and 4-HVA at $m/z$ 117.0557 based on comparison of retention time and fragment spectra to an authentic standard compound or to the hydrolysis product of GVL.

This pattern aligns with the trends observed in the ^{1}H NMR spectrum. Similarly, the FTIR spectrum of DL (*Figure 7*) displays OH vibration signals between 3400 and 3200 cm^{-1}, CH vibration signals at 2962, 2930, 2916 and 2872 cm^{-1}, and carboxylate group signals at 1561 and 1406 cm^{-1}. [49] Although the concentration of sodium 4-hydroxyvalerate is higher than the concentration of depolymerization products in DL, additional signals at 1773 and 1707 cm^{-1} indicates the presence of depolymerization products. The signal at 1770 cm^{-1} can be attributed to conjugated ester groups [50] and the signal at 1707 cm^{-1} can be attributed to the carbonyl group of sodium levulinate, indicating that sodium levulinate is the primary product of lignin depolymerization. The remaining functional groups of levulinate correspond to those of 4-hydroxyvalerate.

The hydrolysis product (sodium 4-hydroxyvalerate) and DL products were characterized using liquid chromatography coupled with electrospray ionization high resolution mass spectrometry (LC-ESI(-)-HRMS). The resulting chromatogram (XIC) of the hydrolysis product (*Figure 8(A)*) shows the signal of the 5 µM GVL standard and the product at $m/z$ 101.0597 (±5 ppm) in positive mode. The GVL standard showed a peak at 1.51 min which could not be detected in the product. Instead, another peak with the same $m/z$ at 1.25 min was observed matching to the [M-H2O]+ ion of 4-hydroxyvaleric acid (4-HVA) with <5 ppm. The absence of the peak of GVL in the product indicated a high conversion rate to the product. The [M-H+]- ion of GVL was not detectible in ESI(-) (*Figure 8 (B)*). In contrast a prominent peak in ESI(-) at $m/z$ 117.0557 was observed in the product, which accurately matches the molecular mass of 4-HVA ([M-H+]-) with a mass deviation <1 ppm (*Figure 8 (C)*).

The resulting extracted ion chromatogram (XIC) of the product of depolymerization shows the signal of the [M-H+]-

ion of a standard of levulinic acid and the product at $m/z$ 115.0400 (±5 ppm) in negative ionization mode (*Figure 9A*). The displayed peak in the product matches with the retention time of the levulinic acid standard. The detection of levulinic acid in the product was supported by comparison of the fragmentation spectra between product and standard. The presence of 4-hydroxyvalerate could also be confirmed by LC-MS (*Figure 9B*) using the hydrolysis product of γ-Valerolactone as reference which was tentatively identified as 4-hydroxvalerate (*Figure 8*). No aromatic compounds could be detected by LC-UV (280 nm).

Sodium levulinate could not be detected in any NMR experiment investigating the stability of GVL (*Figure S4-S6 and S9-S14)*. However, with the aid of mass spectrometry, it was possible to detect a small amount of sodium levulinate in the absence of lignin (*Figure 8)*. Since sodium levulinate has already been detected as a product during the depolymerization of soda lignin in an aqueous Na2CO3 solution, [16] it can be assumed that in this case, the component is formed from both GVL and soda lignin. Compared to the other signals of the DL, those of the sodium levulinate are clearly more intense. Hence, sodium levulinate is assumed as the main product of the depolymerization of soda lignin in GVL and Na2CO3 with the help of a carbon working electrode.

Furthermore, it can be assumed that 4-hydroxyvalerate is formed from soda lignin in addition to levulinate. Hence, both GVL and soda lignin are sources of 4-hydroxyvalerate, [16] which means that the concentration of 4-hydroxyvalerate from the soda lignin can be enriched by the solvent GVL.

## CONCLUSION

The bioelectrorefinery concept amalgamates biorefinery and electrocatalysis, creating a potential avenue for a bio-

based platform chemical. In this investigation, renewable energy is approached as the driving force to convert lignin into aliphatic organic chemicals, while valorizing γ-valerolactone (GVL) as a solvent medium. In summary, this study explored the reductive depolymerization and dearomatization of soda lignin in GVL. Although GVL does not strictly qualify as a reaction-inert solvent, its specific application in ring-opening reactions was emphasized. The focus was on synthesizing valuable bulk chemicals via lignin depolymerization process, enriched by GVL's ring-opening products. Electrochemical depolymerization and dearomatization of soda lignin in GVL produced key compounds like sodium levulinate and sodium 4-hydroxyvalerate. The successful synthesis of bulk chemicals through lignin depolymerization showcases the methodology's potential in chemical manufacturing, contributing to the expansion of *Green Chemistry* and offering innovative pathways for renewable resource utilization, thus promoting the sustainable evolution of the chemical industry. This study enhances the bioelectrorefinery concept, offering novel prospects for harnessing renewable resources and contemplating a viable shift away from crude oil as the predominant source of carbon-based chemicals in industries.

## AUTHOR INFORMATION

### Corresponding Author

*Adam Slabon - Chair of Inorganic Chemistry;
Email slabon@uni-wuppertal.de
*Bruno V. M. Rodrigues - Chair of Inorganic Chemistry;
Email manzolli@uni-wuppertal.de

## ACKNOWLEDGMENT

## REFERENCES

(1) Sheldon, R. A. Engineering a More Sustainable World through Catalysis and Green Chemistry. *J. R. Soc. Interface* **2016**, *13* (116), 20160087. https://doi.org/10.1098/rsif.2016.0087.

(2) Arndt, J.-D.; Freyer, S.; Geier, R.; Machhammer, O.; Schwartze, J.; Volland, M.; Diercks, R. Rohstoffwandel in der chemischen Industrie. *Chem. Ing. Tech.* **2007**, *79* (5), 521–528. https://doi.org/10.1002/cite.200700025.

(3) Lei, L.; Wang, Y.; Zhang, Z.; An, J.; Wang, F. Transformations of Biomass, Its Derivatives, and Downstream Chemicals over Ceria Catalysts. *ACS Catal.* **2020**, *10* (15), 8788–8814. https://doi.org/10.1021/acscatal.0c01900.

(4) Behr, A.; Seidensticker, T. *Einführung in die Chemie nachwachsender Rohstoffe: Vorkommen, Konversion, Verwendung*; Springer Berlin Heidelberg: Berlin, Heidelberg, 2018. https://doi.org/10.1007/978-3-662-55255-1.

(5) Sun, Z.; Fridrich, B.; De Santi, A.; Elangovan, S.; Barta, K. Bright Side of Lignin Depolymerization: Toward New Platform Chemicals. *Chem. Rev.* **2018**, *118* (2), 614–678. https://doi.org/10.1021/acs.chemrev.7b00588.

(6) Li, C.; Zhao, X.; Wang, A.; Huber, G. W.; Zhang, T. Catalytic Transformation of Lignin for the Production of Chemicals and Fuels. *Chem. Rev.* **2015**, *115* (21), 11559–11624. https://doi.org/10.1021/acs.chemrev.5b00155.

(7) Stöcker, M. Biofuels and Biomass-To-Liquid Fuels in the Biorefinery: Catalytic Conversion of Lignocellulosic Biomass Using Porous Materials. *Angew. Chem. Int. Ed.* **2008**, *47* (48), 9200–9211. https://doi.org/10.1002/anie.200801476.

(8) Ansari, K. B.; Arora, J. S.; Chew, J. W.; Dauenhauer, P. J.; Mushrif, S. H. Fast Pyrolysis of Cellulose, Hemicellulose, and Lignin: Effect of Operating Temperature on Bio-Oil Yield and Composition and Insights into the Intrinsic Pyrolysis Chemistry. *Ind. Eng. Chem. Res.* **2019**, *58* (35), 15838–15852. https://doi.org/10.1021/acs.iecr.9b00920.

(9) Strassberger, Z.; Prinsen, P.; Klis, F. V. D.; Es, D. S. V.; Tanase, S.; Rothenberg, G. Lignin Solubilisation and Gentle Fractionation in Liquid Ammonia. *Green Chem.* **2015**, *17* (1), 325–334. https://doi.org/10.1039/C4GC01143K.

(10) Katahira, R.; Mittal, A.; McKinney, K.; Chen, X.; Tucker, M. P.; Johnson, D. K.; Beckham, G. T. Base-Catalyzed Depolymerization of Biorefinery Lignins. *ACS Sustainable Chem. Eng.* **2016**, *4* (3), 1474–1486. https://doi.org/10.1021/acssuschemeng.5b01451.

(11) Chaudhary, R.; Dhepe, P. L. Solid Base Catalyzed Depolymerization of Lignin into Low Molecular Weight Products. *Green Chem.* **2017**, *19* (3), 778–788. https://doi.org/10.1039/C6GC02701F.

(12) Da Cruz, M. G. A.; Gueret, R.; Chen, J.; Piątek, J.; Beele, B.; Sipponen, M. H.; Frauscher, M.; Budnyk, S.; Rodrigues, B. V. M.; Slabon, A. Electrochemical Depolymerization of Lignin in a Biomass-based Solvent. *ChemSusChem* **2022**, *15* (15), e202201246. https://doi.org/10.1002/cssc.202201246.

(13) Oh, H.; Choi, Y.; Shin, C.; Nguyen, T. V. T.; Han, Y.; Kim, H.; Kim, Y. H.; Lee, J.-W.; Jang, J.-W.; Ryu, J. Phosphomolybdic Acid as a Catalyst for Oxidative Valorization of Biomass and Its Application as an Alternative Electron Source. *ACS Catal.* **2020**, *10* (3), 2060–2068. https://doi.org/10.1021/acscatal.9b04099.

(14) Breiner, M.; Zirbes, M.; Waldvogel, S. R. Comprehensive Valorisation of Technically Relevant Organosolv Lignins via Anodic Oxidation. *Green Chem.* **2021**, *23* (17), 6449–6455. https://doi.org/10.1039/D1GC01995C.

(15) Fang, Z.; Flynn, M. G.; Jackson, J. E.; Hegg, E. L. Thio-Assisted Reductive Electrolytic Cleavage of Lignin β-O-4 Models and Authentic Lignin. *Green Chem.* **2021**, *23* (1), 412–421. https://doi.org/10.1039/D0GC03597A.

(16) Lindenbeck, L. M.; Barra, V. C.; Dahlhaus, S.; Brand, S.; Wende, L.; Beele, B. B.; Schebb, Nils. H.; Rodrigues, B. V. M.; Slabon, A. Organic Chemicals from Wood: Selective Depolymerization and Dearomatization of Lignin via Aqueous Electrocatalysis. *ChemSusChem* **2024**, e202301617. https://doi.org/10.1002/cssc.202301617.

(17) Latsuzbaia, R.; Bisselink, R. J. M.; Crockatt, M.; van der Waal, J. C.; Goetheer, E. L. V. Biomass Processing via Electrochemical Means. In *Biomass Valorization*; John Wiley & Sons, Ltd, 2021; pp 225–264. https://doi.org/10.1002/9783527825028.ch8.

(18) Yang, L.; Yuan, H.; Yang, Y.; Wang, R.; Wang, C.; Wei, X.; Chen, S.; Yu, J.; Ma, X. Enhanced Lignin Degradation in Tobacco Stalk Composting with Inoculation of White-Rot Fungi Trametes Hirsuta and Pleurotus Ostreatus. *Waste Biomass Valorization* **2020**, *11* (7), 3525–3535. https://doi.org/10.1007/s12649-019-00692-z.

(19) Hyde, K. D.; Xu, J.; Rapior, S.; Jeewon, R.; Lumyong, S.; Niego, A. G. T.; Abeywickrama, P. D.; Aluthmuhandiram, J. V. S.; Brahamanage, R. S.; Brooks, S.; Chaiyasen, A.; Chethana, K. W. T.; Chomnunti, P.; Chepkirui, C.; Chuankid, B.; De Silva, N. I.; Doilom, M.; Faulds, C.; Gentekaki, E.; Gopalan, V.; Kakumyan, P.; Harishchandra, D.; Hemachandran, H.; Hongsanan, S.; Karunarathna, A.; Karunarathna, S. C.; Khan, S.; Kumla, J.; Jayawardena, R. S.; Liu, J.-K.; Liu, N.; Luangharn, T.; Macabeo,

A. P. G.; Marasinghe, D. S.; Meeks, D.; Mortimer, P. E.; Mueller, P.; Nadir, S.; Nataraja, K. N.; Nontachaiyapoom, S.; O'Brien, M.; Penkhrue, W.; Phukhamsakda, C.; Ramanan, U. S.; Rathnayaka, A. R.; Sadaba, R. B.; Sandargo, B.; Samarakoon, B. C.; Tennakoon, D. S.; Siva, R.; Sriprom, W.; Suryanarayanan, T. S.; Sujarit, K.; Suwannarach, N.; Suwunwong, T.; Thongbai, B.; Thongklang, N.; Wei, D.; Wijesinghe, S. N.; Winiski, J.; Yan, J.; Yasanthika, E.; Stadler, M. The Amazing Potential of Fungi: 50 Ways We Can Exploit Fungi Industrially. *Fungal Diversity* **2019**, *97* (1), 1–136. https://doi.org/10.1007/s13225-019-00430-9.

(20) Coconi Linares, N.; Fernández, F.; Loske, A. M.; Gómez-Lim, M. A. Enhanced Delignification of Lignocellulosic Biomass by Recombinant Fungus *Phanerochaete Chrysosporium* Overexpressing Laccases and Peroxidases. *Microb. Physiol.* **2018**, *28* (1), 1–13. https://doi.org/10.1159/000485976.

(21) Salem, M. Z. M.; Mansour, M. M. A.; Elansary, H. O. Evaluation of the Effect of Inner and Outer Bark Extracts of Sugar Maple ( *Acer Saccharum* Var. *Saccharum* ) in Combination with Citric Acid against the Growth of Three Common Molds. *J. Wood Chem. Technol.* **2019**, *39* (2), 136–147. https://doi.org/10.1080/02773813.2018.1547763.

(22) Spence, E. M.; Scott, H. T.; Dumond, L.; Calvo-Bado, L.; Di Monaco, S.; Williamson, J. J.; Persinoti, G. F.; Squina, F. M.; Bugg, T. D. H. The Hydroxyquinol Degradation Pathway in Rhodococcus Jostii RHA1 and *Agrobacterium* Species Is an Alternative Pathway for Degradation of Protocatechuic Acid and Lignin Fragments. *Appl. Environ. Microbiol.* **2020**, *86* (19), e01561-20. https://doi.org/10.1128/AEM.01561-20.

(23) Barton, N.; Horbal, L.; Starck, S.; Kohlstedt, M.; Luzhetskyy, A.; Wittmann, C. Enabling the Valorization of Guaiacol-Based Lignin: Integrated Chemical and Biochemical Production of Cis,Cis-Muconic Acid Using Metabolically Engineered Amycolatopsis Sp ATCC 39116. *Metab. Eng.* **2018**, *45*, 200–210. https://doi.org/10.1016/j.ymben.2017.12.001.

(24) Conde, J. J.; González-Rodríguez, S.; Chen, X.; Lu-Chau, T. A.; Eibes, G.; Pizzi, A.; Moreira, M. T. Electrochemical Oxidation of Lignin for the Simultaneous Production of Bioadhesive Precursors and Value-Added Chemicals. *Biomass Bioenergy* **2023**, *169*, 106693. https://doi.org/10.1016/j.biombioe.2022.106693.

(25) Klein, J.; Waldvogel, S. R. Selective Electrochemical Degradation of Lignosulfonate to Bio-Based Aldehydes. *ChemSusChem* **2023**, *16* (8), e202202300. https://doi.org/10.1002/cssc.202202300.

(26) Lindenbeck, L.; Liu, Y.; Beele, B. B.; Slabon, A.; Rodrigues, B. V. M. Sustainable Routes for the Depolymerization of Lignocellulosic Biomass. In *Encyclopedia of Inorganic and Bioinorganic Chemistry*; Scott, R. A., Ed.; Wiley, 2023; pp 1–19. https://doi.org/10.1002/9781119951438.eibc2862.

(27) Schotten, C.; Nicholls, T. P.; Bourne, R. A.; Kapur, N.; Nguyen, B. N.; Willans, C. E. Making Electrochemistry Easily Accessible to the Synthetic Chemist. *Green Chem.* **2020**, *22* (11), 3358–3375. https://doi.org/10.1039/D0GC01247E.

(28) Little, R. D.; Moeller, K. D. Introduction: Electrochemistry: Technology, Synthesis, Energy, and Materials. *Chem. Rev.* **2018**, *118* (9), 4483–4484. https://doi.org/10.1021/acs.chemrev.8b00197.

(29) Minteer, S. D.; Baran, P. Electrifying Synthesis: Recent Advances in the Methods, Materials, and Techniques for Organic Electrosynthesis. *Acc. Chem. Res.* **2020**, *53* (3), 545–546. https://doi.org/10.1021/acs.accounts.0c00049.

(30) Horn, E. J.; Rosen, B. R.; Baran, P. S. Synthetic Organic Electrochemistry: An Enabling and Innately Sustainable Method. *ACS Cent. Sci.* **2016**, *2* (5), 302–308. https://doi.org/10.1021/acscentsci.6b00091.

(31) Anastas, P.; Eghbali, N. Green Chemistry: Principles and Practice. *Chem. Soc. Rev.* **2009**, *39* (1), 301–312. https://doi.org/10.1039/B918763B.

(32) May, A. S.; Biddinger, E. J. Strategies to Control Electrochemical Hydrogenation and Hydrogenolysis of Furfural and Minimize Undesired Side Reactions. *ACS Catal.* **2020**, *10* (5), 3212–3221. https://doi.org/10.1021/acscatal.9b05531.

(33) Garedew, M.; Lin, F.; Song, B.; DeWinter, T. M.; Jackson, J. E.; Saffron, C. M.; Lam, C. H.; Anastas, P. T. Greener Routes to Biomass Waste Valorization: Lignin Transformation Through Electrocatalysis for Renewable Chemicals and Fuels Production. *ChemSusChem* **2020**, *13* (17), 4214–4237. https://doi.org/10.1002/cssc.202000987.

(34) Ding, Y.; Greiner, M.; Schlögl, R.; Heumann, S. A Metal-Free Electrode: From Biomass-Derived Carbon to Hydrogen. *ChemSusChem* **2020**, *13* (16), 4064–4068. https://doi.org/10.1002/cssc.202000714.

(35) Dier, T. K. F.; Rauber, D.; Durneata, D.; Hempelmann, R.; Volmer, D. A. Sustainable Electrochemical Depolymerization of Lignin in Reusable Ionic Liquids. *Sci. Rep.* **2017**, *7* (1), 5041. https://doi.org/10.1038/s41598-017-05316-x.

(36) Reichert, E.; Wintringer, R.; Volmer, D. A.; Hempelmann, R. Electro-Catalytic Oxidative Cleavage of Lignin in a Protic Ionic Liquid. *Phys. Chem. Chem. Phys.* **2012**, *14* (15), 5214. https://doi.org/10.1039/c2cp23596j.

(37) Marino, D. D.; Stöckmann, D.; Kriescher, S.; Stiefel, S.; Wessling, M. Electrochemical Depolymerisation of Lignin in a Deep Eutectic Solvent. *Green Chem.* **2016**, *18* (22), 6021–6028. https://doi.org/10.1039/C6GC01353H.

(38) Pollet, P.; Davey, E. A.; Ureña-Benavides, E. E.; Eckert, C. A.; Liotta, C. L. Solvents for Sustainable Chemical Processes. *Green Chem.* **2014**, *16* (3), 1034–1055. https://doi.org/10.1039/C3GC42302F.

(39) Breeden, S. W.; Clark, J. H.; Macquarrie, D. J.; Sherwood, J. Green Solvents. In *Green Techniques for Organic Synthesis and Medicinal Chemistry*; Zhang, W., Cue, B. W., Eds.; Wiley, 2012; pp 241–261. https://doi.org/10.1002/9780470711828.ch9.

(40) Mellmer, M. A.; Sener, C.; Gallo, J. M. R.; Luterbacher, J. S.; Alonso, D. M.; Dumesic, J. A. Solvent Effects in Acid-Catalyzed Biomass Conversion Reactions. *Angew. Chem. Int. Ed.* **2014**, *53* (44), 11872–11875. https://doi.org/10.1002/anie.201408359.

(41) Zhao, X.; Zhou, Z.; Luo, H.; Zhang, Y.; Liu, W.; Miao, G.; Zhu, L.; Kong, L.; Li, S.; Sun, Y. γ-Valerolactone-Introduced Controlled-Isomerization of Glucose for Lactic Acid Production over an Sn-Beta Catalyst. *Green Chem.* **2021**, *23* (7), 2634–2639. https://doi.org/10.1039/D1GC00378J.

(42) Valentini, F.; Brufani, G.; Di Erasmo, B.; Vaccaro, L. γ-Valerolactone (GVL) as a Green and Efficient Dipolar Aprotic Reaction Medium. *Curr. Opin. Green Sustainable Chem.* **2022**, *36*, 100634. https://doi.org/10.1016/j.cogsc.2022.100634.

(43) Kerkel, F.; Markiewicz, M.; Stolte, S.; Müller, E.; Kunz, W. The Green Platform Molecule Gamma-Valerolactone – Ecotoxicity, Biodegradability, Solvent Properties, and Potential Applications. *Green Chem.* **2021**, *23* (8), 2962–2976. https://doi.org/10.1039/D0GC04353B.

(44) González, G.; Ehman, N.; Felissia, F. E.; Area, M. C. Strategies towards a Green Solvent Biorefinery: Efficient Delignification of Lignocellulosic Biomass Residues by Gamma-Valerolactone/Water Catalyzed System. *Ind. Crops Prod.* **2023**, *205*, 117535. https://doi.org/10.1016/j.indcrop.2023.117535.

(45) Umland, J.; Witkowski, S. Notes - Reaction of Silver 4-Hydroxyvalerate with Bromine. *J. Org. Chem.* **1957**, *22* (3), 345–346. https://doi.org/10.1021/jo01354a618.

(46) Wong, C. Y. Y.; Choi, A. W.-T.; Lui, M. Y.; Fridrich, B.; Horváth, A. K.; Mika, L. T.; Horváth, I. T. Stability of Gamma-Valerolactone under Neutral, Acidic, and Basic Conditions. *Struct. Chem.* **2017**, *28* (2), 423–429. https://doi.org/10.1007/s11224-016-0887-6.

(47) Granatier, M.; Schlapp-Hackl, I.; Lê, H. Q.; Nieminen, K.; Pitkänen, L.; Sixta, H. Stability of Gamma-Valerolactone under Pulping Conditions as a Basis for Process Optimization and Chemical Recovery. *Cellulose* **2021**, *28* (18), 11567–11578. https://doi.org/10.1007/s10570-021-04243-5.

(48) Wang, T.; Tao, L.; Zhu, X.; Chen, C.; Chen, W.; Du, S.; Zhou, Y.; Zhou, B.; Wang, D.; Xie, C.; Long, P.; Li, W.; Wang, Y.; Chen, R.; Zou, Y.; Fu, X.-Z.; Li, Y.; Duan, X.; Wang, S. Combined Anodic and Cathodic Hydrogen Production from Aldehyde Oxidation and Hydrogen Evolution Reaction. *Nat. Catal.* **2021**, *5* (1), 66–73. https://doi.org/10.1038/s41929-021-00721-y.

(49) Hadžija, O.; Špoljar, B. Quantitative Determination of Carboxylate by Infrared Spectroscopy: Application to Humic Acids. *Fresenius J. Anal. Chem.* **1995**, *351* (7), 692–693. https://doi.org/10.1007/BF00323352.

(50) Silverstein, R. M.; Webster, F. X.; Kiemle, D. J.; Bryce, D. L. *Spectrometric Identification of Organic Compounds*, Eighth edition.; Wiley: Hoboken, NJ, 2015.